Nuclear Receptor Research
vol. 4 (2017), Article ID 101311, 16 pages
doi:10.11131/2017/101311

AgiAl Publishing House
http://www.agialpress.com/

Research Article

Design of Novel Compounds with the Potential of Dual PPARγ/α Modulation for the Management of Metabolic Syndrome

Claire Ellul and Claire Shoemake

Department of Pharmacy, University of Malta, Msida MSD 2080, Malta

Abstract. This study sought to identify a single molecule capable of managing all three manifestations of metabolic syndrome–hyperglycaemia, dyslipidaemia and hypertension. Two Protein Data Bank (PDB) depositions were selected and used to establish the baseline affinity that any designed molecule in this study should ideally exceed in order to be considered for further optimisation. These were PDB depositions 3VN2 and 2P54 describing the bound co-ordinates of the Peroxisome Proliferator Activated Receptor (PPAR)γ partial agonist and Angiotensin II Receptor (Ang(II)R) blocker telmisartan and of the experimental PPARα fibrate agonist GW590735 bound to their respective cognate receptors. These small molecules were extracted from their cognate receptors, docked into their non-cognate counterparts, conformational analysis performed, and the optimal conformers were selected as template scaffolds in two parallel processes. The first was a fragment based *de novo* approach. Here, molecular moieties from the optimal telmisartan and GW590735 scaffolds modelled in their non-cognate targets and considered critical to binding were identified and modelled, in order to produce seed structures capable of sustaining molecular growth at user-directed sites designated as *H.spc* atoms subsequent to their being docked within the non-cognate Ligand Binding Pockets (LBPs). The second approach was a Virtual Screening (VS) exercise. Here, the optimal telmisartan and GW590735 conformers were submitted as query molecules to VS databases both individually and in the form of a consensus pharmacophore. This VS exercise identified structurally diverse molecules which were electronically and spatially similar to the queries and which were capable of modulating the target receptors. The molecular cohorts identified through both VS and the *de novo* approaches were filtered for Lipinski Rule compliance. The molecules that survived filtering were then re-docked into the non-cognate PPARα and/or γ_LBPs, conformational analysis re-performed and the affinity of the optimal conformer measured for its cognate receptor quantified. Comparison was made to the baseline and non-cognate receptor affinities previously established, and the molecules exhibiting dual affinities exceeding baseline values were selected for further optimisation. The use of the "tried and tested" Ang(II)R blocker and fibrate scaffolds as templates predisposes to the identification of novel structures devoid of unacceptable toxicity.

Keywords: PPAR, Structure-Multiple Activity Relationships

Corresponding Author
Claire Shoemake
claire.zerafa@um.edu.mt

Editor
John Bruning

Dates
Received 20 September 2017
Accepted 20 November 2017

1. Introduction

PPARs are ligand-activated transcription factors. They belong to the nuclear hormone receptor superfamily, and comprise three subtypes: PPARα, PPARγ, and PPARβ/δ. Specifically, PPARα

activation results in triglyceride level reduction. Furthermore, it has been demonstrated that PPARα is involved in in glucose homeostasis and the development of insulin resistance [1]. Activation of the PPARβ/δ receptor results in modification of the body's energy fuel preference from glucose to fat [2]. The PPARγ subtype is a strong inducer of adipogenesis and is involved in glucose metabolism [1]. This means that the PPAR family of nuclear receptors as a whole is a regulator of energy homeostasis and metabolism. PPAR agonism consequently has potential in a wide spectrum of pathologies including adipocyte differentiation, cancer, diabetes, dyslipidaemia, inflammation, lung diseases, neurodegenerative disorders, reproductive disorders, obesity and pain.

Quite a number of ligands, both natural and synthetic, are able to activate the PPAR receptor; these are mostly used in the treatment of glucose and lipid disorders. Literature indicates that, the Polyunsaturated Fatty Acids (PUFAs) γ-linolenic, eicosatrienoic, dihomo-γ-linolenic, arachidonic acid and eicosapentaenoic acid (EPA) interact most efficiently with PPARγ followed by PPARβ/δ. With respect to PPARα, PUFAs do not appear to bind any better than saturated and monounsaturated FAs with the same carbon lengths. EPA may function as the natural endogenous ligand of the PPARs owing to the fact that it shows promiscuity, binding well to all the PPAR subtypes [3]. An exemplar of an endogenous ligand for PPARγ is the oxidized fatty acid 13-hydroxyoctadeca-9,11-dienoic acid (13-HODE).

The bile pigment bilirubin was recently identified as a PPARα agonist at the PPARα receptor. It was shown to reduce both glucose and body fat levels when in rodent experiments. This explains why increased bilirubin levels such as occurs in patients suffering from Gilberts Syndrome appears to have a protective effect on the vascular system [4].

The main PPARγ synthetic full agonists studied to date were the thiazolidinedione (TZD) insulin-sensitizing drugs (e.g. rosiglitazone and pioglitazone) which were withdrawn from the market due to their pharmacovigilance identified undesired adverse effects such as weight gain, oedema [5], bone loss and congestive heart failure [6].

Telmisartan was designed and developed as an Angiotensin II type 1 Receptor (Ang(II)R) Blocker and consequently as an antihypertensive agent. Its promiscuity at PPARγ was coincidental and its allied beneficial clinical consequences serendipitous. Its partial agonism of PPARγ is of utility in the management of cardiometabolic disorders and Type 2 Diabetes Mellitus [7].

The experimental inverse agonist at the PPARγ receptor SR10171 has been associated with the advantage of normalizing metabolic parameters whilst also increasing the turnover of trabecular and cortical bone. This is an important finding owing to the fact that the TZDs are known to cause osteoporosis as a side effect. The bone protective ability of SR10171 has been explained on a molecular level. Specifically it has been attributed to the interactions forged between SR10171 and the PPARγ_LBP where it blocks the activity of phosphorylated Ser^{273} which is associated with osteoclastic activities but not phosphorylated Ser^{112} that has osteoblastic effects [8].

The synthetic fibrates which are a class of triglyceride lowering drugs are ligands for PPARα and are used in the treatment of hypertriglyceridaemia [5]. The active metabolites of the fibrates show preferential binding to the PPARγ receptor subtype, a 10-fold selectivity over the PPARα receptor subtype [1].

The multi-target approach is particularly relevant with the PPARs. Given that PPARα agonism is associated with dislipidaemia management, and that PPARγ agonists have demonstrably been shown to have a potent hypoglycaemic effect, the development of dual α and γ agonists is particularly interesting owing to the fact that dyslipidaemia and diabetes are commonly co-morbid. The fact that the Ang(II)R blocker telmisartan is known to bind to, and act as an agonist at PPARγ, makes the premise of dual PPAR α and γ agonism even more relevant owing to the fact that dual agonists bearing the sartan scaffold could, potentially, target the diabetes, hypercholesterolaemia, and hypertension characteristic of the highly prevalent metabolic syndrome.

2. Methodology

A total of 70 crystallographic depositions describing PPAR receptor isoforms in the *apo-* and *holo-* form were identified in the PDB at the time of study (Nov 2012). The suitability of each PDB crystallographic deposition was assessed for inclusion. A total of 67 PDB entries with resolution of up to 3Å were considered acceptable.

The following crystallographic depositions were chosen as baseline for this study; 3VN2 [9] describing the bound co-ordinates of the partial agonist telmisartan to the PPARγ_LBP, 2P54 [10] describing the experimental fibrate GW590735 bound to PPARα and 2VST [11] where the endogenous ligand 13-hydroxyoctadecadienoic acid (13-HODE) is bound to PPARγ. Another pdb crystallographic deposition, 4ZUD [12] describing the bound co-ordinates of olmesartan to the Ang(II)R was also used in order to assess whether the PPARα and γ modulators identified in this study through the *de novo* and Virtual Screening (VS) drug design processes, would also be able to modulate the Ang(II)R and consequently validate the hypothesis of a single entity capable of managing metabolic syndrome. PROCHECK® [13] was used in order to assess the integrity of these selected depositions.

Molecular modelling was carried out in Sybyl-X® [14]. The small molecules bound to 67 recruited *holo-* systems were extracted from their LBP and their affinity for their respective LBP quantified in X-SCORE® [15]. This allowed calculation for an average LBA (p*K*d) for each PPAR subtype.

The partial PPARγ agonist and Ang(II)R blocker telmisartan and the PPARα agonist GW590735 were the template molecules used in this study. These were docked into their non-cognate PPAR_LBPs and conformational analysis carried out in Sybyl-X® [14]. The optimal conformer in each case was selected based on a combination of high LBA (p*K*d) and low LBE (Kcalmol^{-1}) based on the premises of high affinity and molecular stability. These optimal conformations were used in parallel processes.

3. *de novo* Drug Design

In the *de novo* drug design process, the optimal telmisartan and GW590735 conformers identified through conformational analysis, were used as starting scaffolds for seed structure design. Five seeds, two deriving from the telmisartan scaffold, and three deriving from the GW590735 scaffold were modelled in Sybyl-X® [14]. Seed design was guided by two sources of data; Structure Activity Relationships data available in the literature and critical interactions forged by

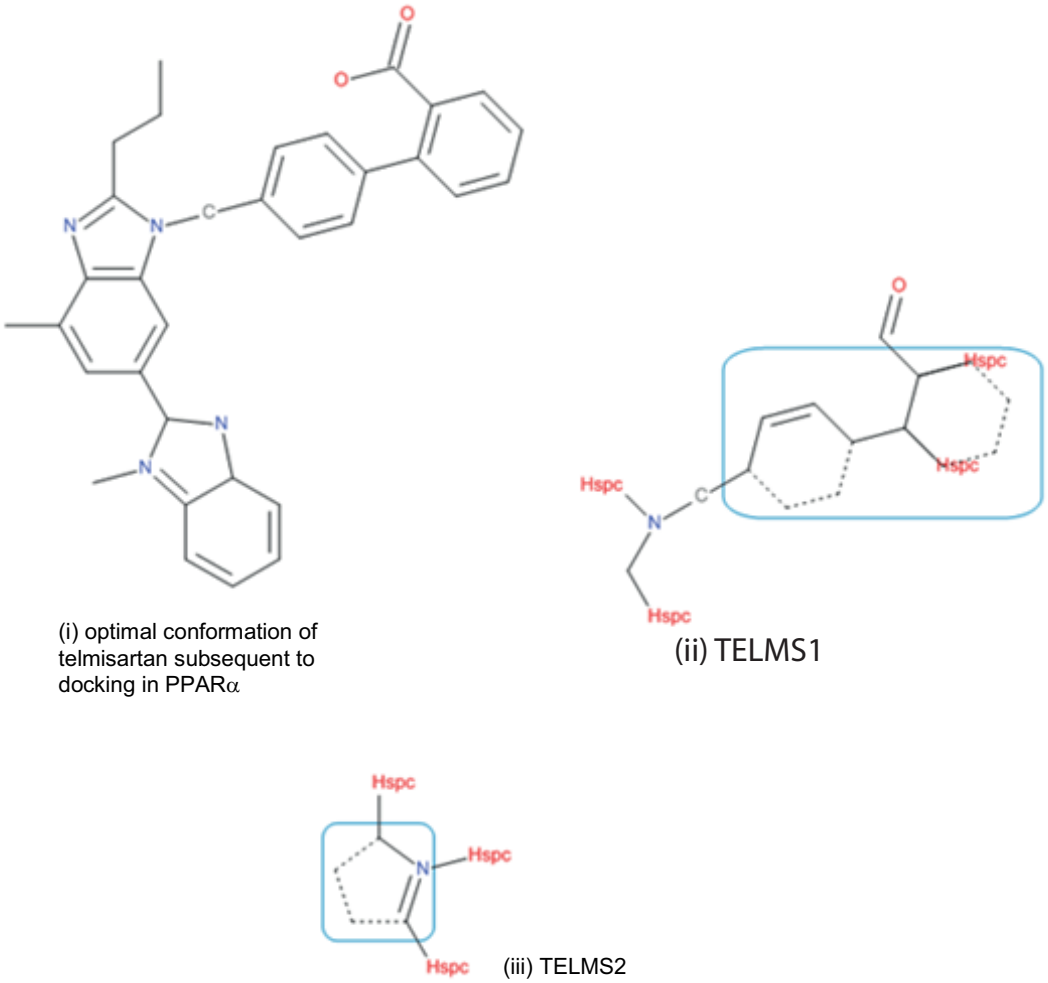

Figure 1: Modelled seed structures derived from the telmisartan scaffold (i) the optimal telmisartan conformer in the non-cognate PPARα_LBP (2P54); (ii) TELMS1 shows the conserved part of the biphenyl moiety in a blue box; (iii) TELMS2 shows in a blue box the preserved part of the nitrogen substituted fused 5-membered ring. Structures rendered in Accelrys® [18].

the small molecules in the respective LBP as elucidated through the generation of 2D topology maps as generated in PoseView® [16]. In each case, molecular growth was user directed. This means that novel moiety introduction was allowed at pre-designated growing sites, modelled in Sybyl-X® [14] through the assignment of *H.spc* hydrogen atoms (highlighted in red font in Figures 1 and 2 respectively) which were recognised by the LINK and GROW modules of LigBuilder® [17] as appropriate anchorage points.

The POCKET module of LigBuilder® version 1.2 [17] was used for LBP mapping and general pharmacophore generation. PDB crystallographic depositions 3VN2 and 2P54 [9, 10] describing the bound co-ordinates of telmisartan bound to PPARγ and of GW590735 bound to PPARα were used to generate LBP maps and general pharmacophoric structures that described the pharmacophoric space circumscribed by telmisartan and GW590735 when these were docked in their cognate and non-cognate LBPs. The surface volume ($Å^3$) of each generated LBP map was quantified in UCSF Chimera® [19].

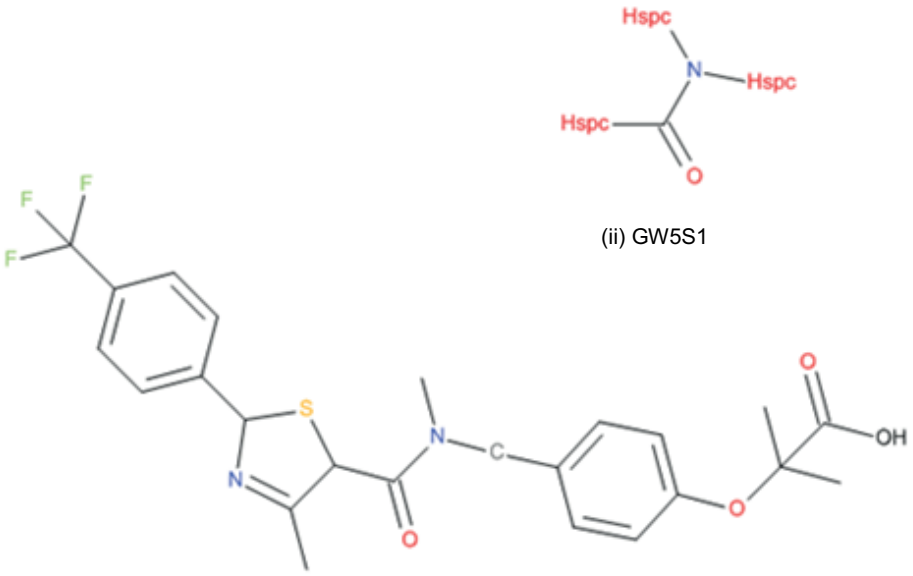

(ii) GW5S1

(i) optimal conformation of GW590735 subsequent to docking in PPARγ

(iv) GW5S3

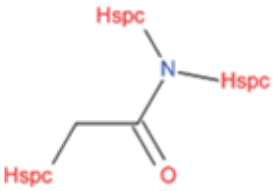

(iii) GW5S2

Figure 2: Modelled seed structures derived from the GW590735 scaffold (i) the optimal GW590735 conformer in the non-cognate PPARγ_LBP (3VN2); (ii) GW5S1 and (iii) GW5S2 preserved the central O-linked spacer portion; (iv) GW5S3 conserved the terminal portions of the molecule (the dotted part was removed). Structures rendered in Accelrys® [18].

Both telmisartan based seed structures, TELMS1 and TELMS2 and two out of three GW590735 based seed structures specifically GW5S1 and GW5S2 were, as depicted in Figures 1 and 2 designed to sustain terminal growth. For all of these seed structures, the GROW module of LigBuilder® version 1.2 [17] was invoked to drive the *de novo* design process. The GW590735 based seed structure GW5S3 was essentially composed of two disconnected molecular fragments. For this seed structure *de novo* molecular growth was sustained in the LINK module of LigBuilder® version 1.2 [17]. Execution of the GROW and LINK algorithms resulted in the elaboration of a series of molecules that required further schematic organization.

Implementation of the PROCESS algorithm of LigBuilder® version 1.2 [17] for each molecular cohort that was generated for each seed structure resulted in the creation of a molecular database that contained molecules which were segregated according to pharmacophoric similarity and which were ranked according to LBA (p*K*d). The molecular databases also contained physicochemical information which included general formula, molecular weight, clogP, and a

chemical score that was indicative of synthetic feasibility. The contents of each generated molecular database (n=5) for each of the modeled seed structures considered in this study were further filtered using Lipinski rule compliance [20] as inclusion criteria. Five molecules were selected from each molecular cohort (n=5). Selection was made according to binding affinity and clogP values. Molecules of varying clogP were selected, making sure that a spectrum of molecules whose clogP was skewed towards hydrophilicity and lipophilicity respectively was included. Specifically, molecules with clogP values that ranged from 1 to ≤4 were considered to be mostly hydrophilic and therefore more likely to be targeted for central compartment associated conditions, whereas molecules with clogP values that ranged from 4 to ≤5 were considered to be mostly lipophilic and consequently able to target peripheral compartment associated conditions [21]. The chosen molecules were then subjected to conformational analysis in Sybyl-X® [14]. Specifically, all the selected structures deriving from the seed structures TELMS1 and TELMS2 were docked into the PPARγ_LBP (pdb ID 3VN2) while selected structures deriving from GW5S1, GW5S2 and GW5S3 were docked into the PPARα_LBP (pdb ID 2P54). In each case, the best conformer was chosen, as previously explained, based on having a combination of highest LBA (pKd) and lowest LBE (Kcalmol^{-1}). The LBA (pKd) of the best conformers were then compared to the precalculated values, specifically the average affinity of all the *holo*-systems calculated in the first part of the study, as well as to the affinities of telmisartan and 13-HODE for the PPARγ_LBP and GW590735 for the PPARα_LBP respectively (refer to Table 2 in results section).

The critical interactions of the optimal conformations of the selected molecules with their corresponding receptor were visualised in PoseView® [16]. Their hydrophilic and hydrophobic interactions were then compared to those obtained through similar analysis of the pdb crystallographic depositions that were used as baselines for this study specifically 3VN2 [9] and 2P54 [10] describing the bound co-ordinates of telmisartan with PPARγ and GW590735 with PPARα respectively. This process was carried out in the interest of identifying dual modulators for the PPARγ/α subtype.

4. Virtual Screening

The optimal telmisartan and GW590735 conformers obtained subsequent to docking into the non-cognate PPARα and γ_LBPs were submitted to the database ViCi® [22] for the identification of sterically and electronically similar structures. MONA®, [23], a cheminformatics platform which facilitates compound library processing was used in order to filter the two molecular cohorts obtained from the molecular database ViCi® [22] for Lipinski Rule compliance.

Sybyl-X®'s v1.1 [14] Surflex-dock^{TM} algorithm was then invoked in order to generate two protomols for the pdb crystallographic depositions that were used as baseline for this study. The *holo*- complexes pdb ID 3VN2 [9] describing the bound co-ordinates of telmisartan with PPARγ, and pdb ID 2P54 [10] describing the bound co-ordinates of GW590735 with PPARα were successively loaded into Sybyl-X® v1.1 [14]. All unnecessary moieties including the bound small molecule (telmisartan and GW590735 respectively), and non-critical water molecules were removed consequently creating two *apo*- proteins. A set-up file for each protomol was created; this contained the necessary information to guide small molecule docking to the protomol. The filtered molecular cohorts emanating from MONA® [23] when the best

conformers of telmisartan and GW590735 in the PPARα and γ_LBPs respectively together with nine decoy molecules were docked back into their respective protomols and ranked in order of affinity. 10 molecules from each cohort were chosen based on favorable scores obtained from the various methods employed and physicochemical properties.

Two consensus pharmacophores were generated in LigandScout® 4.0 [24]. The first was an average of the telmisartan co-ordinates as co-crystallised with PPARγ (pdb ID 3VN2) [9] and its optimal conformer docked within the PPARα_LBP. The second was an average of GW590735 as those of its co-crystallised within the PPARα_LBP (pdb ID 2P54) [10] and its optimal conformer docked within the PPARγ_LBP respectively. These consensus pharmacophores were submitted sequentially to ZINCPharmer® [25]. During the VS process using ZINCPharmer® [25], a number of stringent filters were enforced in order to allow for molecular optimization by structural modification, while remaining within Lipinski's [20] recommendations for ensuring bioavailability. Other criteria proposed by Veber and his co-workers [26] suggest that orally bioavailable molecules should have 10 or fewer rotatable bonds and a low polar surface area ($<140\text{Å}^2$) or total hydrogen bond count (<12 hydrogen bond donors and acceptors). Therefore, a molecular weight of 200-250 and 1-3 rotatable bonds for the first consensus pharmacophore submitted to ZINCPharmer® [25] were used as filtering criteria, however for the second consensus pharmacophore submitted, the criteria for molecular weight had to be widened to 200-500. The molecular cohorts identified from the ZINCPharmer® [25] database were read into the previously generated protomols. Specifically, the Lipinski rule compliant molecules obtained after submitting the molecular pair telmisartan:optimal telmisartan conformer in PPARα consensus pharmacophore were docked in the protomol generated for 3VN2 [9] whereas the molecules that were obtained after submitting the GW590735:optimal GW590735 in PPARγ consensus pharmacophore pair to ZINCPharmer® [25] were docked in the protomol created for 2P54 [10] in Sybyl-X®'s [14] docking suite, respectively. Each molecular cohort subsequent to docking into its respective protomol, the molecules were ranked in order of binding affinity to the protomol.

Three molecules from each molecular cohort were chosen based on favorable scores and physicochemical properties.

Molecules that predisposed towards dual PPARγ/α modulation were docked into the *apo-* Ang(II)R_LBP as described in pdb crystallographic deposition 4ZUD [12] where the bound small molecule olmesartan is cognate. Conformational analysis was performed for each selected molecule and the optimal conformer identified, again based on high LBA (pKd) and low LBE (Kcalmol^{-1}). These results were compared to the LBA (pKd) of olmesartan to its cognate Ang(II)R as described in pdb crystallographic deposition 4ZUD [12] and to the LBA (pKd) of telmisartan subsequent to it being docked in the Ang(II)R. 2D topology maps of the critical interactions of the optimal conformations of the selected molecules within the Ang(II)R were generated in PoseView® [16]. Their hydrophilic and hydrophobic interactions were then compared to those obtained through similar analysis of pdb crystallographic deposition 4ZUD [12] that was used as baseline for this study and to the interactions forged by the optimal telmisartan conformer when this was docked into the Ang(II)R as described in pdb crystallographic deposition 4ZUD [12].

The potential of the selected molecules to act as PPARγ inverse agonists in a manner analogous to the experimental molecule SR10171 was also assessed [8]. To this aim, when these were docked into the PPARγ_LBP, the key interactions forged between them and the amino

Table 1: The surface volume in Å^3 occupied by the molecules that were selected as baseline in this study, telmisartan and GW590735 in the cognate and non-cognate PPARα and γ_LBPs quantified in UCSF Chimera® [19].

	Surface Volume (Å^3)		
	Cognate	**Non-cognate**	**Protomol**
Telmisartan	640.5	646.2	-
Protomol (telmisartan in cognate PPARγ_LBP as described in pdb crystallographic deposition 3VN2)	-	-	1273
GW590735	646.6	626.8	-
Protomol (GW590735 in cognate PPARα_LBP as described in pdb crystallographic deposition 2P54)	-	-	1145

acids lining the LBP were assessed in order to identify whether or not any interactions were being forged between these molecules and phosphorylated Ser^{273} and Ser^{112}.

Chosen molecules which apart from being able to act as dual PPARγ/α modulators also showed LBAs (p*K*d) similar to those of olmesartan and telmisartan towards the Ang(II)R were submitted to the webserver ProTox [27] in order to predict their oral toxicity in rodents.

5. Results and Discussion

As indicated previously, a total of 70 *apo*- and *holo*- PPAR related crystallographic depositions were identified from the pdb at the time of study (November 2012). 67 of these were identified as suitable for this study; a resolution of up to 3Å was considered suitable for a pdb crystallographic deposition to be included in the study. All four Ramachandran plots generated in PROCHECK [13], for the pdb crystallographic depositions that were chosen as baseline for this study had most residues, that is more than 90%, in the most favoured regions of the plot which further reinforced their suitability as template crystallographic depositions.

Comparison was made of the surface volume (Å^3) of the LBP maps generated in LigBuilder® [17] when the cognate and non-cognate small molecules telmisartan and GW590735 were docked. The fact that this volume remained largely constant across the board as shown in Table 1 implies the spatial similarity from a volume perspective of the two PPAR subtypes considered and also of the magnitude of the two high affinity ligands used as templates for this study. This molecular volume similarity also bodes well for the design, as this study aims to do, of dual PPAR γ/α modulators and potentially established volume requirements for such molecules.

The volume of the protomol, the idealized LBP generated through identification of the energetically disfavoured space at the core of the PPAR subtypes, was of 1273Å^3 and 1145Å^3 for PPARγ and PPARα as described in pdb crystallographic depositions 3VN2 and 2P54 respectively. These volumes are significantly larger that the LBP maps described in LigBuilder® [4]. This is not surprising given that the algorithms in the two software programmes (LigBuilder® and Sybyl-X®) used are not the same, and that they calculate different variables. In the case of LigBuilder® [17], calculation is made based on direct contact between the ligand and the surrounding amino acids while in Sybyl-X® [14] the protomol is calculated as a function of the energetically unsatisfied amino acids within a 0.5Å^3 region of the docked ligand. The latter necessarily describes a larger volume which represents a greater but not necessarily bioactive space for design.

The general structure of PPAR agonists is documented in the literature [28]; the general structure of PPARα specific fibrates is also well documented [29]. Specifically, PPAR agonism has been associated with the molecular existence of an acidic head group, a short linker to an aromatic ring and a second linker to a cyclic tail which can be an aromatic or an aliphatic ring system. Fibrates which are PPARα specific agonists also fall into this broad generalisation.

The molecules designed *de novo* in this study, as well as those identified through VS which complied with Lipinski's Rules and that fell into a clogP range that predicted different *in vivo* distribution based on polarity, were analysed for conformity to these documented structural pre-requisites.

GW5S2_F2S115, generated *de novo* from the GW5S2 molecular cohort, seen in Figure 3(i), possesses an acidic head group linked to an aromatic centre and a tail that is not cyclic. The naphthalene group with the butyl side chain in GW5S2_F2S115 is similar to the central benzimidazole group with the propyl side chain of telmisartan.

Molecule 509 that was identified through VS using the online molecular database ViCi® [22], seen in Figure 3(ii) when the best conformer of telmisartan in the non-cognate PPARα was submitted as query molecule has an acidic group that lies centrally in the molecule. The multiple aromatic rings that constitute structure 509 make it resemble molecule GW590735 that was used as baseline in this study.

Molecule ZN4, shown in Figure 3(iii), that was identified through VS using the online molecular database ZINCPharmer® [25], when the consensus pharmacophore generated between the molecular pair GW590735:best GW590735 conformer in PPARγ was submitted as query molecule also conforms to the general structure proposed for PPAR agonists. The quinolone and benzothiazole groups in molecule ZN4 are similar to the two benzimidazole groups that constitute telmisartan.

When the interactions forged between telmisartan and its cognate PPARγ_LBP were compared to those forged between the optimal GW590735 conformer and the non-cognate PPARγ_LBP, the following similarities were observed:

- A hydrogen bond arises between Tyr^{473} and the centrally located benzimidazole group in telmisartan and the thiazole group in GW590735.
- Non-polar interactions arising from Cys^{285} and Met^{364} were observed with the acidic head groups of both telmisartan and GW590735.

When the interactions forged between GW590735 and its cognate PPARα_LBP were compared to those forged between the optimal telmisartan conformer and the non-cognate PPARα_LBP, similar interactions were also observed. These included:

- Hydrogen bonds between the acidic head groups of both molecules and residues Tyr^{314}, His^{440} and Tyr^{464} of the PPARα_LBP.
- Non-polar interactions between Cys^{275}, Cys^{276}, Val^{332} and Met^{355} and the PPARα_LBP were observed when both molecules were resident.

Molecule GW5S2_F2S115 (ref to Figure 3(i)) showed dual PPARγ/α affinity. Compound GW5S2_F2S115 forged a hydrogen bond between a carbonyl group and Tyr^{473} similar to telmisartan. Another hydrogen bond was forged with Ser^{289} in the PPARγ_LBP. His^{323} and Ser^{289}

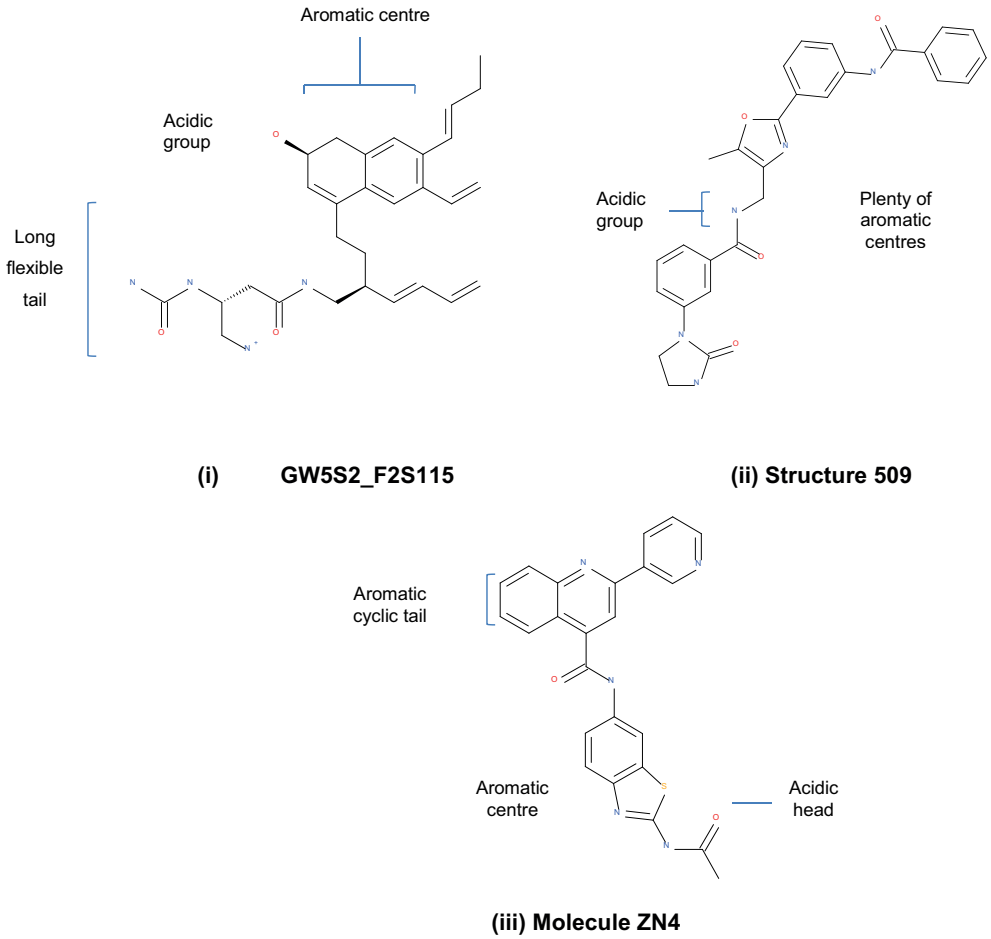

Figure 3: 2D representation of (i) GW5S2_F2S115, (ii) structure 509 and (iii) molecule ZN4, generated through VS using the online molecular database ZINCPharmer® [25] when the consensus pharmacophore derived from the molecular pair GW590735: best GW590735 conformer in PPARγ was submitted as query molecule. Rendered in Accelrys® [18].

were involved in hydrogen bonding interactions when interactions forged between PPARγ full agonists were observed.

Non-polar interactions with Cys^{285} and Met^{364} were forged between GW5S2_F2S115 and the PPARγ_LBP. Hydrophobic interactions help to stabilise the PPARγ_LBP and are similar to those cited in the literature for interactions forged by partial agonists with the PPARγ_LBP [29]. These interactions were also forged when telmisartan was in its cognate PPARγ_LBP.

When GW5S2_F2S115 was re-docked into the PPARα_LBP, hydrogen bonds with Ser^{280}, Tyr^{314}, His^{440} and Tyr^{464} were forged between the selected molecule, and the PPARα_LBP. Non-polar interactions with Cys^{275} and Met^{355} were also observed. These interactions were the same as those observed when GW590735 was in its cognate PPARα_LBP as described in pdb crystallographic deposition 2P54 [10].

Molecule 509 (ref to Figure 3(ii)) forged two hydrogen bonds; one between a basic carbonyl and Cys^{275} (ref to Figure 6(i)) and the other located centrally in the molecule with Met^{355} of the PPARα_LBP. Molecule number 509 forged polar interactions between a basic carbonyl group and Cys^{285} and the other between the oxygen of an oxazole group in the molecule and His^{449} when this was docked in the PPARγ_LBP. On the other hand, only one hydrogen bond was

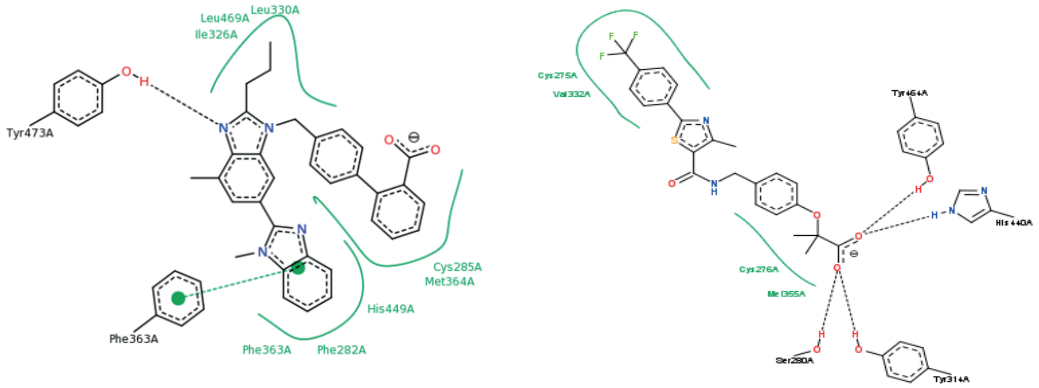

(i) Telmisartan **(ii) GW590735**

Key:	Colour	Type of interaction
	Green dotted line	Pi-stacked
	Black dotted line	Hydrogen Bond
	Green smooth contour lines	Hydrophobic

Figure 4: Critical interactions forged by (i) the PPARγ partial agonist telmisartan and by (ii) the PPARα experimental fibrate agonist GW590735 with the PPARγ and α_LBPs of pdb crystallographic depositions 3VN2 [9] and 2P54 [10] respectively. Generated in PoseView® [16].

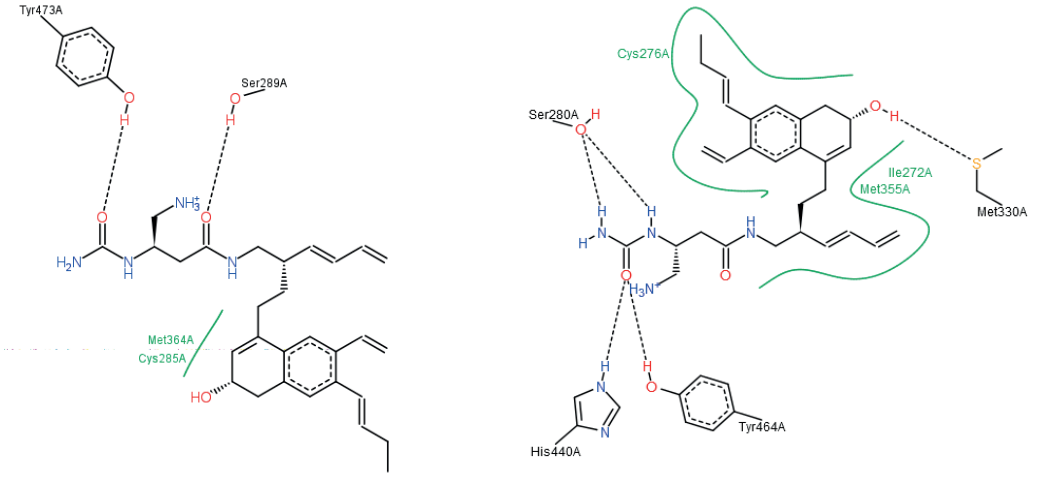

(i) **(ii)**

Key:	Colour	Type of interaction
	Green dotted line	Pi-stacked
	Black dotted line	Hydrogen Bond
	Green smooth contour lines	Hydrophobic

Figure 5: 2D topology maps of molecule GW5S2_F2S115 docked in the (i) PPARγ and (ii) α_LBPs as described in pdb crystallographic depositions 3VN2 [2] and 2P54 [3] respectively. Generated in PoseView® [13].

forged between the central benzimidazole group of telmisartan and Tyr^{473} within the cognate PPARγ_LBP.

Two pi-pi stacked interactions with residues Phe^{363} and Phe^{282} were forged between molecule number 509 and the PPARγ_LBP as described in pdb crystallographic deposition 3VN2 [9]. The

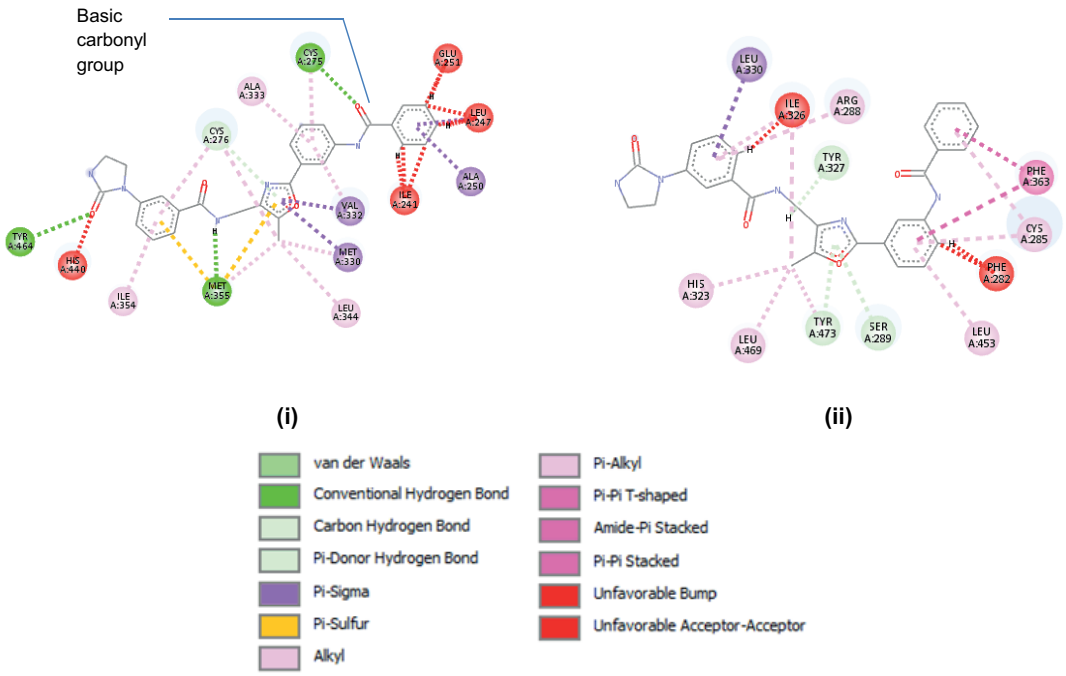

Figure 6: Critical contacts forged between molecule 509 identified through VS when the optimal telmisartan conformer in the non-cognate PPARα_LBP was planted within the (i) PPARα and (ii) PPARγ_LBPs as described in pdb crystallographic depositions 2P54 [10] and 3VN2 [9] respectively. Generated in Discovery Studio® [30].

pi-pi stacked interaction with the terminal benzene ring and Phe^{363} is similar to that observed between telmisartan's terminal benzimidazole and the PPARγ_LBP. Non-polar interactions at both molecule termini were observed with Phe^{282}, Phe^{363} and Met^{364} similar to telmisartan in the PPARγ_LBP [2]. The similarity in the interactions forged by molecule 509 to telmisartan in the PPARγ_LBP may make this structure a partial agonist at the named receptor.

Reference is made to the molecular cohort identified through VS using the online molecular database ZINCPharmer® [25] when consensus pharmacophore GW590735:optimal GW590735 in the PPARγ_LBP was submitted as a query molecule. The only identified molecule, referred to as molecule ZN4 in this study, showed dual PPAR γ/α affinity. When molecule ZN4 (ref to Figure 3(iii)) was docked in the PPARγ_LBP, a conventional hydrogen bond was forged between a central acidic nitrogen and Ser^{289}. In telmisartan a similar hydrogen bond between a basic nitrogen on the central benzimidazole group and Tyr^{473} was forged in the cognate PPARγ_LBP. Non-polar interactions with Met^{364} and Cys^{285} were forged, similarly to the partial agonist telmisartan interactions in PPARγ_LBP. A pi-pi stacked interaction with Phe^{282} was also present, similar to the pi-pi stacked interaction forged between telmisartan's terminal benzimidazole and Phe^{363} lining the PPARγ_LBP [9]. Docking of compound ZN4 into the PPARα_LBP resulted in the forging of conventional hydrogen bonds with Tyr^{314} and Tyr^{464}, pi-sulfur interactions with Met^{330} and Met^{355} similar to the interactions forged by GW590735 and the cognate PPARα_LBP [10].

None of the chosen molecules that were selected as optimal and thus suitable for further optimization, specifically GW5S2_F2S115 derived *de novo* from the GW5S2 molecular cohort, molecule 509 identified through VS using the online molecular database ViCi® [22] when the best conformer of telmisartan in PPARα was submitted as query molecule and molecule ZN4

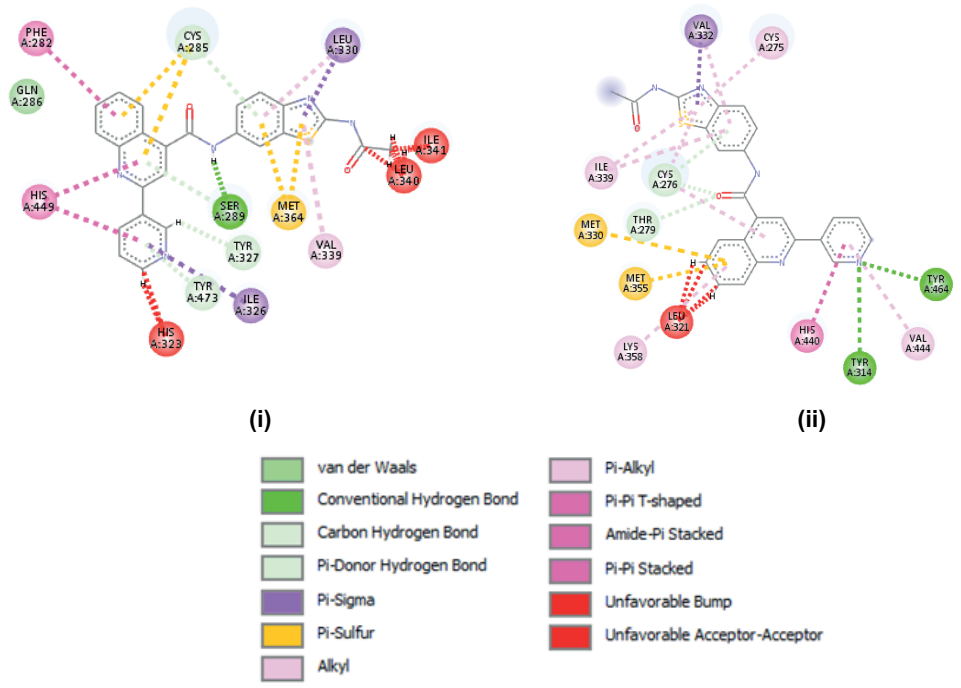

Figure 7: Critical contacts forged between molecule ZN4 identified through VS when the consensus pharmacophore derived from the molecular pair GW590735:optimal GW590735 conformer in the non-cognate PPARγ_LBP was submitted as query molecule docked within the (i) PPARα and (ii) PPARγ_LBPs as described in pdb crystallographic depositions 2P54 [9] and 3VN2 [10] respectively. Generated in Discovery Studio® [30].

identified through VS using the searchable molecular database ZINCPharmer® [25] when the consensus pharmacophore derived from GW590735: best GW590735 conformer in PPARγ was submitted as query molecule were shown to forge any interactions with phosphorylated Ser^{273} and Ser^{112}.

The post-translational modifications occurring subsequent to ligand binding, that result in dephosphorylation of Ser^{112} and Ser^{273} of the PPARγ_LBP result in pro-adipocytic and insulin-sensitizing effects respectively [31]. The molecules identified in this study consequently do not appear to have potential in the management of osteoporosis.

The premise of the design of novel structures with the functional ability to simultaneously manage the three conditions; hypertension, hypercholesterolaemia and diabetes inherent to metabolic syndrome must be addressed.

When there is excessive caloric intake, there is a metabolic overload that results in an increase in triglyceride input which causes adipocyte enlargement. In obese, non-diabetic subjects, TG storage and β-oxidation in muscle are normally maintained to prevent insulin resistance. However, upon further excessive caloric intake, adipocytes undergo hypertrophy with the resultant increase in the secretion of macrophage chemoattractants. This results in a pro-inflammatory state where TG deposition is impaired and lipolysis is increased; resulting in an increase in circulating FFA and TG that accumulate in skeletal muscle, liver and β -cells to form long chain fatty acyl co-A esters that disrupt normal metabolic and secretory functions of these tissues. The inflammatory response thus contributes to metabolic dysfunction in obesity [32].

In the case of PPARα, defective fatty acid metabolism can result in the development of non-alcoholic fatty liver disease [33].

Table 2: The LBAs (p*K*d) of telmisartan and GW590735 for their cognate and non-cognate receptors (red font) and the LBAs (p*K*d) of 13-HODE and olmesartan. The average LBAs (p*K*d) calculated from the 3 *holo*- PPAR complexes deposited on the pdb (Nov 2012) are included as a reference.

	Preferred IUPAC name, rendered in MarvinSketch 17.13 [36]	**LBA (pKd)**			
		PPAR isoform			
		δ	γ	α	**Ang(II)R**
Average for all ligands in the PDB crystallographic depositions considered acceptable in this study		7.79	7.92	7.94	
13-HODE	(9Z,11E,13S)-13-hydroxyoctadeca-9,11-dienoic acid		5.86		
Telmisartan	4'-{[4-methyl-6-(1-methyl-1H-1,3-benzodiazol-2-yl)-2-propyl-1H-1,3-benzodiazol-1-yl]methyl}-[1,1'-biphenyl]-2-carboxylic acid		9.26	7.16	7.66
GW590735			5.75	7.84	
Olmesartan	4-(2-hydroxypropan-2-yl)-2-propyl-1-{[2'-(1H-1,2,3,4-tetrazol-5-yl)-[1,1'-biphenyl]-4-yl]methyl}-1H-imidazole-5-carboxylic acid				7.08

Cytokines such as TNFα cause a downregulation of PPARγ and related target genes which result in excessive adipose tissue and obesity with its related problems. However, the use of PPARγ agonists was shown to suppress local TNFα production [34].

This has to be kept in mind when designing novel molecules that might be able to modulate the PPARγ and α receptors especially, in the case of fibrates that are predominant PPARα agonists, whose metabolites show preferential binding to PPARγ.

Body weight and adiposity regulation by fenofibrate is regulated by sexual dimorphism. Oestrogen was found to compete with the co-activator binding site of PPARα, therefore inhibiting the actions of PPARα in obese females with functioning ovaries [35].

The two approaches adopted in this study, specifically *de novo* design and VS yielded 1 molecule and 2 molecules (GW5S2_F2S115, 509 and ZN4) respectively with the *in silico* calculated affinity attributes (molecule GW5S2_F2S115 LBA (p*K*d) for PPARγ = 9.45; LBA (p*K*d) for PPARα = 7.47; structure 509 LBA (p*K*d) for PPARγ = 8.44; LBA (p*K*d) for PPARα = 7.73; molecule ZN4 LBA (p*K*d) for PPARγ = 7.46; LBA (p*K*d) for PPARα = 7.72) that predisposed towards dual PPARγ/α agonism. These molecules were subsequently docked into the Ang(II)R_LBP as described in pdb ID 4ZUD [11] in which the bound small molecule was olmesartan. As previously outlined, telmisartan, and molecules GW5S2_F2S115, structure 509 and molecule ZN4 were docked into the olmesartan bound Ang(II)R_LBP and conformational analysis performed. This was done in order to assess the LBA of these molecules for the Ang(II)R and assess their ability to also mitigate hypertension. The LBA of the optimal conformer of each of the four molecules was selected as representative and their LBA selected for comparison. Reference is made to Table 2 where it is evident that the optimal conformations of molecules GW5S2_F2S115, structure 509 and molecule ZN4 bind to the Ang(II)R with an

in silico calculated affinity (p*K*d 6.51, 6.89 and 6.68) that is comparable to that of the optimal conformation of telmisartan (p*K*d=7.66) at this locus.

Molecules GW5S2_F2S115 and molecule ZN4 showed predicted class IV oral toxicity (harmful is swallowed). However, this result is comparable to that obtained for telmisartan. Structure 509 exhibited class III oral toxicity in rodents (toxic if swallowed), which is comparable to the toxicity of olmesartan. The two baseline molecules 13-HODE and GW590735 showed class V and VI oral toxicities respectively and are therefore the least toxic.

The toxicity of the selected *de novo* and virtually identified molecules was, as previously stated assessed using ProTox [27].These toxicity evaluations seem to indicate that GW5S2_F2S115 and compounds 509 and ZN4 are toxic if orally ingested, a fact that would pose serious limitations on the future investment value of these molecules. This toxicity assessment must however be viewed in relation to that also made for telmisartan and olmesartan which exhibit similar toxicity predictions and are in current clinical use. The implication consequently is that these molecules would be suitable for oral administration – a premise that requires *in vivo* validation.

Competing Interests

The authors declare no competing interests.

Acknowledgements

This Article is based upon work from COST Action CA15135, supported by COST.

References

[1] B. Grygiel-Górniak, "Peroxisome proliferator-activated receptors and their ligands: nutritional and clinical implications—a review," *Nutrition Journal*, vol. 13, article 17, 2014.

[2] E. Adeghate, A. Adem, M. Y. Hasan, K. Tekes, and H. Kalasz, "Medicinal chemistry and actions of dual and pan PPAR modulators," *The Open Medicinal Chemistry Journal*, vol. 5, no. 2, pp. 93–98, 2011.

[3] H. E. Xu, M. H. Lambert, V. G. Montana et al., "Molecular recognition of fatty acids by peroxisome proliferator-activated receptors," *Molecular Cell*, vol. 3, no. 3, pp. 397–403, 1999.

[4] D. E. Stec, K. John, C. J. Trabbic et al., "Bilirubin binding to PPARα inhibits lipid accumulation," *PLoS ONE*, vol. 11, no. 4, Article ID e0153427, 2016.

[5] B. G. Shearer and W. J. Hoekstra, "Peroxisome Proliferator-Activated Receptors (PPARs): choreographers of metabolic gene transcription," *Cell Transmissions*, vol. 18, no. 3, pp. 3–10, 2002.

[6] M. Ahmadian, J. M. Suh, N. Hah et al., "PPARγ signaling and metabolism: the good, the bad and the future," *Nature Medicine*, vol. 19, no. 5, pp. 557–566, 2013.

[7] S. C. Benson, H. A. Pershadsingh, C. I. Ho et al., "Identification of Telmisartan as a Unique Angiotensin II Receptor Antagonist With Selective PPAR -Modulating Activity," *Hypertension*, vol. 43, no. 5, pp. 993–1002, 2004.

[8] L. Stechschulte, P. Czernik, Z. Rotter et al., "PPARG Post-translational Modifications Regulate Bone Formation and Bone Resorption," *EBioMedicine*, vol. 10, pp. 174–184, 2016.

[9] Y. Amano, T. Yamaguchi, K. Ohno et al., "Structural basis for telmisartan-mediated partial activation of PPAR gamma," *Hypertension Research*, vol. 35, no. 7, pp. 715–719, 2012.

[10] M. L. Sierra, V. Beneton, A. Boullay et al., "Substituted 2-[(4-Aminomethyl)phenoxy]-2-methylpropionic Acid PPARα Agonists. 1. Discovery of a Novel Series of Potent HDLc Raising Agents," *Journal of Medicinal Chemistry*, vol. 50, no. 4, pp. 685–695, 2007.

[11] T. Itoh, L. Fairall, K. Amin et al., "Structural basis for the activation of PPARgamma by oxidized fatty acids," *Nature Structural & Molecular Biology*, vol. 15, no. 9, pp. 924–931, 2008.

[12] H. Zhang, H. Unal, R. Desnoyer et al., "Crystal structure of human angiotensin receptor in complex with inverse agonist olmesartan at 2.8Å resolution," *J Biol Chem*, vol. 290, no. 49, pp. 29127–29139, 2015.

[13] R. A. Laskowski, M. W. MacArthur, D. S. Moss, and J. M. Thornton, "PROCHECK: a program to check the stereochemical quality of protein structures," *Journal of Applied Crystallography*, vol. 26, pp. 283–291, 1993.

[14] SYBYL-X 1.2, Tripos International, 1699 South Hanley Rd., St. Louis, Missouri, 63144, USA.

[15] R. Wang, L. Liu, L. Lai, and Y. Tang, "SCORE: A new empirical method for estimating the binding affinity of a protein-ligand complex," *Journal of Molecular Modeling*, vol. 4, no. 12, pp. 379–394, 1998.

[16] K. Stierand and M. Rarey, "PoseView – molecular interaction patterns at a glance," *Journal of Cheminformatics*, vol. 2, no. Suppl 1, p. P50, 2010.

[17] R. Wang, Y. Gao, and L. Lai, "LigBuilder: A Multi-Purpose Program for Structure-Based Drug Design," *Journal of Molecular Modeling*, vol. 6, no. 7-8, pp. 498–516, 2000.

[18] Accelrys Software Inc. (now Dassault Systèmes), Accelrys Draw, Release 4.0, San Diego: Accelrys Software Inc., 2010.

[19] C. C. Huang, G. S. Couch, E. F. Pettersen, T. E. Ferrin, and Chimera., "An extensible molecular modeling application constructed using standard components," *Pacific Symposium on Biocomputing*, pp. 7–24, 1996.

[20] C. A. Lipinski, F. Lambardo, B. W. Dominy, and P. J. Feeney, "Experimental and computational approaches to estimate solubility and permeability in drug discovery and development settings," *Advanced Drug Delivery Reviews*, vol. 64, supplement, pp. 4–17, 2012.

[21] A. K. Ghose, T. Herbertz, R. L. Hudkins, B. D. Dorsey, and J. P. Mallamo, "Knowledge-based, central nervous system (CNS) lead selection and lead optimization for CNS drug discovery," *ACS Chemical Neuroscience*, vol. 3, no. 1, pp. 50–68, 2012.

[22] V. Lamzin, ViCi - *In-silico* Ligand-based Drug Design. 2016 [cited 2016 Apr 5]. Available from: EMBL Hamburg, http://www.embl-hamburg.de/vici/index.

[23] M. Hilbig, S. Urbaczek, I. Groth, S. Heuser, and M. Rarey, "MONA – Interactive manipulation of molecule collections," *Journal of Cheminformatics*, vol. 5, no. 1, p. 38, 2013.

[24] G. Wolber, A. A. Dornhofer, and T. Langer, "Efficient overlay of small organic molecules using 3D pharmacophores," *Journal of Computer-Aided Molecular Design*, vol. 20, no. 12, pp. 773–788, 2007.

[25] D. R. Koes and C. J. Camacho, "ZINCPharmer: pharmacophore search of the ZINC database," *Nucleic Acids Research*, vol. 40, no. W1, pp. W409–W414, 2012.

[26] D. F. Veber, S. R. Johnson, H.-Y. Cheng, B. R. Smith, K. W. Ward, and K. D. Kopple, "Molecular properties that influence the oral bioavailability of drug candidates," *Journal of Medicinal Chemistry*, vol. 45, no. 12, pp. 2615–2623, 2002.

[27] M. N. Drwal, P. Banerjee, M. Dunkel, M. R. Wettig, and R. Preissner, "ProTox: a web server for the in silico prediction of rodent oral toxicity," *Nucleic Acids Research*, vol. 42, no. W1, pp. W53–W58, 2014.

[28] F. Loiodice and G. Pochetti, "Structural insight into the crucial role of ligand chirality in the activation of PPARs by crystallographic methods," *Current Topics in Medicinal Chemistry*, vol. 11, no. 7, pp. 819–839, 2011.

[29] T. L. Lemke, D. A. Williams, V. F. Roche, and S. W. Zito, *Foyes Principles of Medicinal Chemistry*, Lippincott Williams Wilkins, Philadelphia, 7th edition, 2013.

[30] Dassault Systèmes BIOVIA, *Discovery Studio Modeling Environment*, Dassault Systèmes, San Diego, Release 4.5 edition, 2015.

[31] V. Kolli, L. A. Stechschulte, A. R. Dowling, S. Rahman, P. J. Czernik, and B. Lecka-Czernik, "Partial agonist, telmisartan, maintains PPARγ serine 112 phosphorylation, and does not affect osteoblast differentiation and bone mass," *PLoS ONE*, vol. 9, no. 5, Article ID e96323, 2014.

[32] A. Guilherme, J. V. Virbasius, V. Puri, and M. P. Czech, "Adipocyte dysfunctions linking obesity to insulin resistance and type 2 diabetes," *Nature Reviews Molecular Cell Biology*, vol. 9, no. 5, pp. 367–377, 2008.

[33] A. Montagner, A. Polizzi, E. Fouché et al., "Liver PPARa is crucial for whole-body fatty acid homeostasis and is protective against NAFLD," *Gut*, vol. 65, pp. 1202–1214, 2016.

[34] D. E. Moller and J. P. Berger, "Role of PPARs in the regulation of obesity-related insulin sensitivity and inflammation," *International Journal of Obesity*, vol. 27, no. S3, pp. S17–S21, 2003.

[35] M. Yoon, "PPARα in obesity: sex difference and estrogen involvement," *PPAR Research*, vol. 2010, Article ID 584296, 16 pages, 2010.

[36] MarvinSketch 17.13, 2017, ChemAxon (http://www.chemaxon.com).